Transport control within a microtube

A. Kwang-Hua Chu
Department of Physics, Xinjiang University, Wulumuqi 830046, People's Republic of China
and P. O. Box 30-15, Shanghai 200030, People's Republic of China
(Received 9 February 2004; revised manuscript received 3 May 2004; published 3 December 2004)

Investigation of the entrainment of gases induced by a surface wave propagating along the wall of a microtube is conducted by using a relaxed model with slip velocity boundary conditions. Flow patterns tuned by critical reflux values a_0, Knudsen numbers, Reynolds numbers, and the wave number are demonstrated. Results show that once the cross section of the microtube is narrowed down (slip velocity increasing) there are earlier backward flows and the flow pattern is much more complicated. Our results should be useful for the design of micro total analytical systems.

DOI: 10.1103/PhysRevE.70.061902 PACS number(s): 87.19.St, 87.68.+z, 89.75.Kd, 85.85.+j

I. INTRODUCTION

Integrated microfluidic (μfluidic) devices are being used to automate the generation and analysis of chemical compounds [1,2]. Chemical analyses on μfluidic devices can be highly automated and reduce the consumption of reagents by several orders of magnitude. Miniaturized analysis systems, however, depend on the precise control of fluids through the network. Some approaches, like pressure-driven flows (delivered by, say, micropumps [3,4]), electro-osmotic flows (EOF's), where the circuits use electrophoretic separations [3,5,6], and most recently, surface-acoustic-wave-(SAW-)driven flows [7] (e.g., Love-wave devices incorporating guiding layers of spun polymethylmethacrylate (PMMA) on ST quartz) have been adopted by many researchers. The last method is still in the developing stage and can be related to the previously well-known peristaltic transport in biofluidic applications [8] such as flexible and/or deformable microconduits or microtubes. The control methodology for SAW-driven flows is similar to EOF considering the wall or boundary tuning mechanism; however, the SAW-driven flows escape from the rather large external electric field that is necessary for EOF.

Inspired by nature and current technologies, for example, respiratory mechanisms in insects, we can reconstruct a system for scientific and physiological applications [9]. Most insects respire through a system of tubes (called tracheae) that connect to the air via spiracles that can be actively opened or closed. These tiny tubes are gas-filled vessels (the diameter can be as small as 1 μm) and they function to exchange gas with tissues of the body. One of the possible external mechanisms for respiration is muscle contraction (in the abdomen) [9] which is similar to the peristaltic-wave-driven method [8]: wavy motion along the boundary of tubes induces a streaming flow or reflux along the tube (for a certain range of wave numbers and wave speeds).

We note that rarefied gases flowing in static rigid channels with the dominant physical parameter being the Knudsen number (Kn$=\ell/d$, where ℓ is the mean free path of the gas and d is the width of the channel) have been studied since the late 1870s [10]. Recently researchers have started to investigate slip flow (the regime characterized by $0.001 \leqslant \mathrm{Kn} < 0.15$) within static rigid plane microchannels or microtubes, which are common in microdomains of microelectromechanical system (MEMS) applications [4,11–14], and found certain interesting physical behavior. The nonzero slip velocity normally comes from incomplete momentum transfer along the gas-surface (collision and reflection) boundary when the pressure inside the channel is rather low and also because the characteristic length scale of the cross-sectional geometry is in submicrometers. At present, although a large variety of silicon-based microconduits [12] can be fabricated in a highly controllable and reproducible manner, to achieve a defect-free silicon surface during the fabrication of microtubes [14] (say, the diameter being of the order of magnitude of micrometers) is still a challenge.

We also know, however, that most of the sensors in biomicroelectromechanical systems (bio-MEMS) perform in a wide dynamic range and with high sensitivity [11], which implies that microtubes or nanotubes built in the microstructure of MEMS are easily subjected to environmentally dynamic and random noises [15]. That is to say, the flow rate of gases in microtubes embedded in soft MEMS might be tuned by these dynamic noises even though they might be minor from the macroscopic point of view.

In this study, we shall illustrate possible time-averaged effects due to the boundary (surface) coupling with the inertia of rarefied gases in micro- and nanotubes which may be directly related to rarefied gas flow in μfluidic devices. For simplicity, we shall only consider slow (quasistatic) wave motions which permit us to not take into account real dynamic phenomena [16]. Thus, the details of a possible close-coupled dispersion relation between the (surface) wave number and wave speed will not be considered here and relevant applications of them are beyond our present approach. We obtain flow patterns tuned by the critical reflux (pressure-gradient) values in some range of Reynolds numbers associated with a medium wave number of peristaltic waves propagating along the wall of the microtube. To the best knowledge of the author, considering the present micro- and nanofabrication technologies, and measurement techniques, the experimental side of our results is still unproven. That is to say, the crucial issue is to generate a surface wave experimentally in a precise way, but how to filter out the noise wave within the micro- and nanodomains from the ambient environment is yet unknown. It is also rather difficult to mea-

 ©2004 The American Physical Society

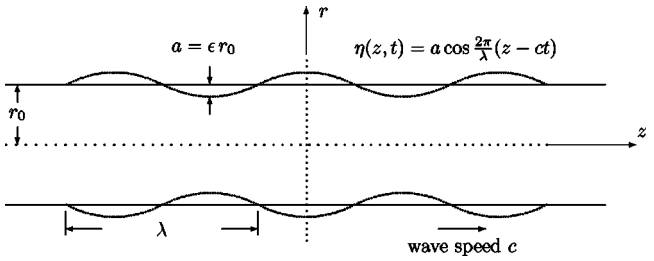

FIG. 1. Schematic longitudinal diagram of the deformable motion of the microtube's wall inside one cross-section with respect to the tube axis (the orientation is counted from, say, the *x* axis which is normal to the *z* axis). The tube is axisymmetric.

sure or visualize the velocity profiles in a micro- or nanodomain, especially for dynamic profiles in a microtube with the cross-section geometry being of the order of magnitude of micrometers. On the other hand, as commented in [17], in microfluidic devices using electro-osmotic flow control, electro-osmosis has proven difficult to apply because the effect is generated by a complex interplay among surface composition, buffer characteristics, and external voltage fields. Transporting minute amounts of material across a surface has resulted in poor flow-control reproducibility. Thus, our approach and relevant results could be useful to researchers in this field.

II. FORMULATIONS

We consider a circular cylindrical (elastic) microtube of uniform thickness filled with a homogeneous rarefied gas. The wall of the tube is not absolutely rigid; on it is imposed axisymmetric traveling sinusoidal waves of moderate amplitude a (z is the axial coordinate in the wave propagation direction). The radial displacement from the mean position of the wall ($r=r_0$) is thus presumed to be η, where $\eta = a\cos[2\pi(z-ct)/\lambda]$, λ is the wavelength, and c is the wave speed. Axisymmetric motion is assumed with r measured in the direction normal to the mean position of the wall (please see Fig. 1). u,v are the velocity components in the z and r directions, respectively.

It would be expedient to simplify these equations by introducing dimensionless variables. We have a characteristic velocity c and three characteristic lengths a, λ, and r_0. The following variables based on c and r_0 could thus be introduced:

$$r' = r/r_0, \quad z' = z/r_0, \quad u' = u/c, \quad v' = v/c,$$

$$\eta' = \eta/r_0, \quad \psi' = \psi/(cr_0^2), \quad t' = (ct)/r_0, \quad p' = p/(\rho c^2).$$

In the following, the primes for the dimensionless variables will be dropped for convenience. The relevant governing equations for an incompressible flow are

$$\nabla \cdot \mathbf{u} = 0, \quad \mathbf{u} \equiv (u,v),$$

$$\partial \mathbf{u}/\partial t + \mathbf{u} \cdot \nabla \mathbf{u} = -\nabla p + \nabla^2 \mathbf{u}/\mathrm{Re}.$$

The amplitude ratio ϵ, the wave number α, and the Reynolds number Re are defined by $\epsilon = a/r_0$, $\alpha = (2\pi r_0)/\lambda$, $\mathrm{Re} = (cr_0)/\nu$. We shall seek a solution in the form of a series in the parameter ϵ: $\psi = \psi_0 + \epsilon\psi_1 + \epsilon^2\psi_2 + \cdots$, $\partial p/\partial z = (\partial p/\partial z)_0 + \epsilon(\partial p/\partial z)_1 + \epsilon^2(\partial p/\partial z)_2 + \cdots$, with $v = (\partial\psi/\partial z)/r$, $u = -(\partial\psi/\partial r)/r$.

The two-dimensional (r and z) momentum equations and the equation of continuity could be in terms of the stream function ψ if the pressure (p) term is eliminated. The final governing equation is

$$\frac{\partial}{\partial t}\hat{\nabla}^2\psi + \frac{\psi_z}{r}\left[\hat{\nabla}^2\psi_r - \frac{2}{r}\hat{\nabla}^2\psi + \frac{\psi_r}{r^2}\right] - \frac{\psi_r}{r}\hat{\nabla}^2\psi_z = \frac{1}{\mathrm{Re}}\hat{\nabla}^4\psi,$$

$$\hat{\nabla}^2 \equiv \frac{\partial^2}{\partial z^2} + \frac{\partial^2}{\partial r^2} - \frac{1}{r}\frac{\partial}{\partial r}, \tag{1}$$

where the subscripts indicate partial differentiation. The fluid is subjected to boundary conditions imposed by the symmetric motion of the wall and the nonzero slip velocity [10,15,18]: $u = -\mathrm{Kn}\, du/dr$, $v = \partial\eta/\partial t$ at $r = (1+\eta)$. $\mathrm{Kn} = \ell/r_0$, where ℓ is the mean free path. The boundary conditions can be expanded in powers of η and then ϵ:

$$\left[\left(\frac{-1}{r}\frac{\partial}{\partial r}\right)(\psi_0 + \epsilon\psi_1 + \epsilon^2\psi_2 + \cdots)\right]\Bigg|_{r=1+\epsilon\cos\alpha(z-t)}$$
$$= -\mathrm{Kn}\left[\left(\frac{1}{r^2}\frac{\partial}{\partial r} - \frac{\partial^2}{r\partial r^2}\right)(\psi_0 + \epsilon\psi_1 + \epsilon^2\psi_2 + \cdots)\right]\Bigg|_{r=1+\epsilon\cos\alpha(z-t)}, \tag{2}$$

$$\psi_{0z}|_1 + \epsilon[\cos\alpha(z-t)\ \psi_{0zr}|_1 + \psi_{1z}|_1]$$
$$+ \epsilon^2\left[\frac{\psi_{0zrr}|_1}{2}\cos^2\alpha(z-t) + \cos\alpha(z-t)\ \psi_{1zr}|_1 + \psi_{2z}|_1\right]$$
$$+ \cdots = -\epsilon\alpha\sin\alpha(z-t) - \epsilon^2\alpha\cos\alpha(z-t)\sin\alpha(z-t). \tag{3}$$

The equations above, together with the condition of symmetry and a uniform pressure gradient in the z direction, $(\partial p/\partial z)_0 = \text{const}$ yield

$$\psi_0 = K_0[(1+2\mathrm{Kn})r^2 - r^4/2], \quad K_0 = (\mathrm{Re}/8)[(\partial p/\partial z)_0], \tag{4}$$

and

$$\psi_1 = \phi(r)e^{i\alpha(z-t)} + \phi^*(r)e^{-i\alpha(z-t)}, \tag{5}$$

where the asterisk denotes the complex conjugate. Similarly, we have

$$\psi_2 = D(r) + E(r)e^{i2\alpha(z-t)} + E^*(r)e^{-i2\alpha(z-t)} \tag{6}$$

and the associated boundary conditions. We consider only the case of $\mathrm{Kn} \gg O(\epsilon)$ from the above boundary conditions, which means the mean free path of the rarefied gas is much larger than the amplitude of the wall-surface wave.

To simplify the approach and obtain preliminary analytical solutions of the above complicated equations and boundary conditions, we shall present the case in which $(\partial p/\partial z)_0$ vanishes or $\psi_0 = 0$ (free pumping cases). This is directly

linked to flow control without an external pressure-driven mechanism.

After lengthy algebraic manipulations, we obtain

$$\phi = A_0 r I_1(\overline{\alpha} r) + B_0 r I_1(\alpha r), \tag{7}$$

where $A = A_0/\mathcal{D}$, $B = B_0/\mathcal{D}$, $\mathcal{D} = [\mathrm{Kn}\overline{\alpha}^2 I_1(\overline{\alpha}) + \overline{\alpha} I_0(\overline{\alpha})] I_1(\alpha) - [\mathrm{Kn}\alpha^2 I_1(\alpha) + \alpha I_0(\alpha)] I_1(\overline{\alpha})$, $A_0 = [\mathrm{Kn}\alpha^2 I_1(\alpha) + \alpha I_0(\alpha)]/2$, $B_0 = -[\mathrm{Kn}\overline{\alpha}^2 I_1(\overline{\alpha}) + \overline{\alpha} I_0(\overline{\alpha})]/2$, and I_n is the modified Bessel function of the first kind of order n.

To obtain a simple solution that relates to the mean flow so long as only terms of $O(\epsilon^2)$ are concerned, we see that if every term in the z-momentum equation is averaged over an interval of time equal to the period of oscillation, we can then obtain (from our solutions as given by the above equations) the mean pressure gradient

$$\overline{(\partial p/\partial z)} = \epsilon^2 \overline{(\partial p/\partial z)_2} + O(\epsilon^3) = \epsilon^2 \left\{ \frac{1}{r\,\mathrm{Re}} \left(- D_{rrr} + \frac{D_{rr}}{r} - \frac{D_r}{r^2} \right) + \frac{i\alpha}{r^2} \left[\phi \phi^*_{rr} - \phi^* \phi_{rr} - \frac{1}{r} (\phi \phi^*_r - \phi^* \phi_r) \right] \right\} + O(\epsilon^3). \tag{8}$$

If fact, as it is similar to the derivation of no-slip cases [8], we have

$$\overline{(\partial p/\partial z)} = \epsilon^2 (a_0/\mathrm{Re}) + O(\epsilon^3) \tag{9}$$

with a_0 an integration constant. In practical applications we must determine a_0 from considerations of the conditions at the ends of the microtube. Once a_0 is specified, our solution for the mean axial velocity (averaged over time) of the flow is

$$U(r) = \epsilon^2 \left\{ - R_0 - \alpha^2\,\mathrm{Re}^2 \left[\left(1 - \mathrm{Kn} \right) G(1) - \frac{G(r)}{r} + \mathrm{Kn} G_r(1) \right) \right] + \frac{a_0}{4} (1 + 2\mathrm{Kn} - r^2) \right\} \tag{10}$$

where $R_0 = -[\phi_{rr}(1) + \phi^*_{rr}(1)]/2$ as $\mathrm{Kn} = 0$, and $G(r)$ is a combination of $\phi(r)$ and its higher order r derivatives.

III. RESULTS AND DISCUSSION

Numerical calculations confirm that the mean streamwise velocity distribution (averaged over time) due to the peristaltic motion in the case of free pumping is dominated by R_0 (or Kn) and the parabolic distribution $-a_0(1-r^2)$. R_0, which defines the boundary value, has its origin in the r gradient of the second-order streamwise velocity distribution, as can be seen in the equations above.

Now let us define the critical reflux condition as one for which the mean velocity $U(r)$ equals zero at the centerline $r=0$. With Eqs. (8)–(10), we have, for the second-order term,

$$a_0 = \mathrm{Re}\,\overline{(\partial p/\partial z)_2}, \tag{11}$$

which means the critical reflux condition is reached when a_0 has this value ($a_{0_{cr}}$). Pumping against a positive pressure gradient greater than the critical value would result in a backward flow (reflux) in the central region of the stream. This critical value depends on α, Re, and Kn. There will be no reflux if the pressure gradient is smaller than this a_0.

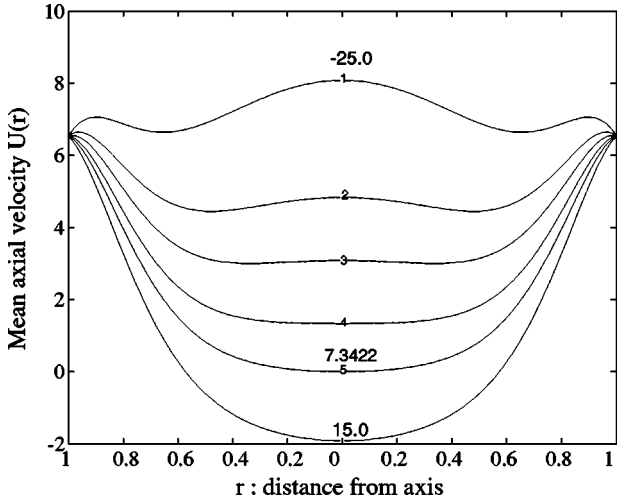

FIG. 2. Dependence of the mean velocity profile $U(r)$ on a_0 for the wave number $\alpha = 0.8$, the Reynolds number $\mathrm{Re} = 50$, $\mathrm{Kn} = 0$. a_0 increases from −25 to 15. $a_{0_{cr}} = 7.3422$ Kn is the Knudsen number (see the text for the definition). a_0 is related to the second-order pressure gradient. All quantities shown here and in subsequent figures are dimensionless.

The physical significance of a_0 is demonstrated in Figs. 2 and 3. The effect of slip velocities (tuned by Kn) with fixed wave number ($\alpha = 0.8$) on $U(r)$ is also demonstrated in these figures for $\mathrm{Re} = 50$ with different a_0 [ranges −25, −12, −5, 2, 7.3422 ($a_{0_{cr}}$), 15 for the no-slip case, Fig. 2, and ranges −25, −12, −5, 2, 5.2303 ($a_{0_{cr}}$), 15 for the slip case, Fig. 3]. All the quantities shown in the figures here are dimensionless. We observe that once there is a slip velocity ($\mathrm{Kn} \neq 0$) along the wall, the flow decoupling from the motion of the peristaltic waves propagating along the wall is larger. This implies that

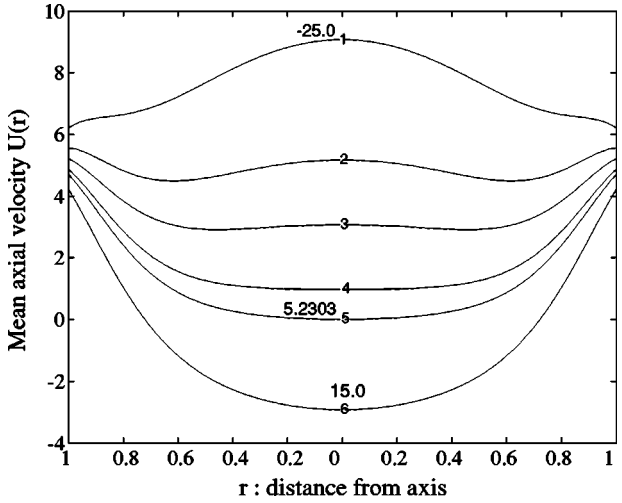

FIG. 3. Dependence of the mean velocity profile $U(r)$ on a_0 for the wave number $\alpha = 0.8$, the Reynolds number $\mathrm{Re} = 50$, $\mathrm{Kn} = 0.1$. a_0 increases from −25 to 15. $a_{0_{cr}} = 5.2303$. As $a_0 = a_{0_{cr}}$, $U(r=0) = 0$, i.e., a backward flow starts to form.

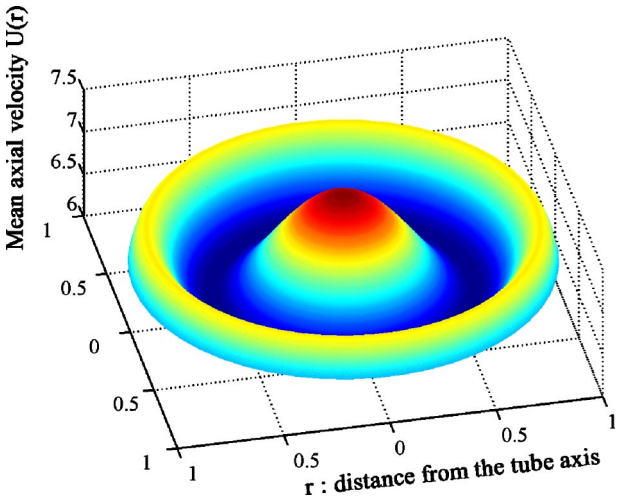

FIG. 4. (Color online) Three-dimensional view of the mean velocity profile $U(r)$ for Re=50, α=0.8, Kn=0, a_0=−22.

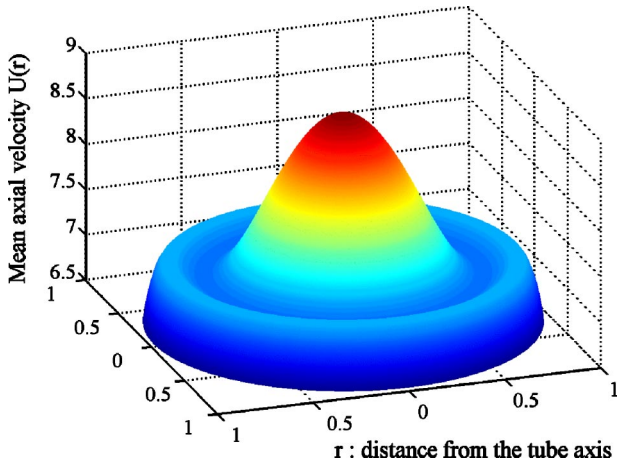

FIG. 5. (Color online) Three-dimensional view of the mean velocity profile $U(r)$ for Re=50, α=0.8, Kn=0, a_0=−28.

flow control in slip flows driven by a peristaltic wave is much more difficult than that in the no-slip case. Once the Reynolds number increases, the nonlinear coupling effect due to the peristaltic wave and the fluid inertia is enhanced. To understand the meaning of flow control, as evidenced in Eq. (10) for U, we can either adjust the values of the small amplitude surface waves (ϵ), the wave number (α), the wave speed (Re), on the physical properties of the fluid and/or the tube (Kn) or tune a_0 to obtain the flow pattern. We must remind the readers that once the physical parameters are prescribed, $a_{0_{cr}}$ is then fixed and unique, and different a_0 will result in different $U(r)$, e.g., either a forward or a reverse flux, as shown here.

In fact, the "control" here is open-loop control, for any stable state (considering ψ_0, since the Reynolds numbers we adopted are rather small here compared to the critical Reynolds number in a similar linear stability analysis for a tube in a no-slip case [19]) of small amplitude (surface) waves, the frequency $\omega=\alpha c$ is not fixed but can be arbitrarily tuned. This implies that α and c are independent variables here. Researchers who use the peristaltic-wave approaches normally treated the wave number α and the wave speed c independently [8]. Insects, however, as noted in Ref. [9], might alter these properties physiologically by either suddenly deforming or narrowing down the microtube's cross section or strengthening/compressing the microtubes (geometrical ways). The latter could change the thickness of the microtubes. As for adjusting c, it could be tuned via the elastic constant of the microtube and its environment or interface. This is related to the softening or hardening of the material of the microtube or its interface/environment. Here, we must remind the readers that the microscopic structure for the material is, in fact, porous. The macroscopic elasticity and/or viscosity could thus be altered through a microscopic change of the porosity or thermal effects around the porous structures which are accessible in insects.

To illustrate the detailed three-dimensional velocity field for different a_0 (−22 and −28 for corresponding $a_{0_{cr}}$ =7.3422) under the same Knudsen number (Kn=0), Reynolds number (Re=50), and peristaltic wave number (α =0.8), we plot $U(r)$ versus r in Figs. 4 and 5. It is clear that once $|a_0|$ becomes small, it is not possible to sustain a completely forward-moving flow relative to the peristaltic (or surface acoustic) wave (propagating along the tube wall).

In fact, the critical reflux values decrease for the slip cases for all ranges of (Re, α). The direct interpretation about this behavior is that once there are slip velocities along the wall, the backward-moving gas flows are much more easily triggered than no-slip ones inside micro- and nanotubes so that the pumping power should be increased at the beginning for stable flow control. Meanwhile, as there are early backward-moving flows due to slip-flow effects, the gas flows might become more unstable than in the previous no-slip cases. Thus a detailed study of gases flowing in deformable micro- or nanotubes should be performed as early as possible for the understanding of respiratory mechanisms [9], flow control in μfluidic devices, and the design of micro total analysis systems [2]. We shall investigate more complicated problems [3,16,20–22] and take into account the viscoelasticity [23] (like that of biological vessels but with slip velocity boundary conditions) in the future. In the latter case, for the viscoelastic medium, the dispersion relation for one-dimensional (1D) surface (transverse) waves proportional to $\exp(i\alpha z - i\omega t)$ can be given as $\rho\omega^2 = K(\omega)\alpha^2$, where ρ is the mass density of the medium and $K(\omega)$ is the frequency-dependent transverse elastic modulus which can also be given in a complex form [24] and is characterized by a relaxation time τ (for $\omega\tau \gg 1$, K recovers the elastic limit). Based on this, the entire formulations will be essentially nontrivial and complicated. Furthermore, the slip velocity boundary conditions for a viscoelastic medium are obscure at present.

ACKNOWLEDGMENTS

The author is partially supported by the National Natural Science Foundation of China (NSFC under Grant No. 10274061) and the China Post-Doctoral Science Foundation (Grant No. 1999-17).

[1] R. B. Schasfoort *et al.*, Science **286**, 942 (1999).
[2] *Micro Total Analysis System*, edited by D. J. Harrison and A. van den Berg (Kluwer, Dordtrecht, 1998).
[3] G. M. Whitesides and A. D. Stroock, Phys. Today **54**(6), 42 (2001).
[4] J. Pfahler, J. Harley, H. H. Bau, and J. Zemel, Sens. Actuators, A **21-23**, 431 (1990).
[5] A. E. Herr *et al.*, Anal. Chem. **72**, 1053 (2000).
[6] R. Qiao and N. R. Aluru, J. Micromech. Microeng. **12**, 625 (2002).
[7] J. W. Grate, B. M. Wise, and N. B. Gallagher, Anal. Chim. Acta **490**, 169 (2003).
[8] F. Yin and Y. C. Fung, J. Appl. Mech. **36**, 579 (1969); K. P. Selverov and H. A. Stone, Phys. Fluids **13**, 1837 (2001); M. Mishra and A. R. Rao, ZAMP. **54**, 532 (2003).
[9] M. W. Westneat, O. Betz, R. W. Blob, K. Fezzaa, W. J. Cooper, and W.-K. Lee, Science **299**, 558 (2003).
[10] M. N. Kogan, *Rarefied Gas Dynamics* (Plenum, New York, 1969).
[11] M. Esashi, K. Minami, and T. Ono, Condens. Matter News **6**, 31 (1998).
[12] K. Komvopoulos, Wear **200**, 305 (1996).
[13] J. P. Shelby, D. S. W. Lim, J. S. Kuo, and D. T. Chiu, Nature (London) **425**, 38 (2003); N. R. Tas, P. Mela, T. Kramer, J. W. Berenschot, and A. van den Berg, Nano Lett. **3**, 1537 (2003).
[14] V. K. Dwivedi, R. Gopal, and S. Ahmad, Microelectron. J. **31**, 405 (2000); D. Brutin and L. Tadrist, Phys. Fluids **15**, 653 (2003).
[15] A. K.-H. Chu, Electron. Lett. **38**, 1481 (2002); A. K.-H. Chu, IEE Proc.: Nanobiotechnol. **150**, 21 (2003).
[16] A. I. Dobrolyubov, *Waves Transfer of Matter* (Belorussian Sciences, Minsk, 1996).
[17] N. A. Polson and M. A. Hayes, Anal. Chem. **73**, 313A (2001).
[18] A. R. Wazzan, R. C. Lind, and C. Y. Liu, Phys. Fluids **11**, 1271 (1968).
[19] W. H. Reid and B. S. Ng, Fluid Dyn. Res. **33**, 5 (2003); A. E. Trefethen, L. N. Trefethen, and P. J. Schmid, Comput. Methods Appl. Mech. Eng. **1926**, 413 (1999).
[20] B. B. Mandelbrot and R. F. Voss, in *Noise in Physical Systems and* $1/f$ *Noise*, edited by M. Savelli, G. Lecoy, and J.-P. Nougier (Elsevier Science, New York, 1983), p. 31.
[21] M. Ueda, H. Oana, Y. Baba, M. Doi, and K. Yoshikawa, Biophys. Chem. **71**, 113 (1998).
[22] M. P. Brenner, L. S. Levitov, and E. O. Budrene, Biophys. J. **74**, 1677 (1998).
[23] M. Gad-el-Hak, Prog. Aerosp. Sci. **38**, 77 (2002).
[24] I. Rudnick, J. Low Temp. Phys. **40**, 287 (1980); B. Gross, *Mathematical Structure of the Theories of Viscoelasticity* (Hermann, Paris, 1953); I. M. Ward, *Mechanical Properties of Solid Polymers* (Wiley, London, 1971).